

# The classical diffusion-limited Kronig-Penney system

D. Bar

**Abstract**

*We have previously discussed the classical diffusive system of the bounded one-dimensional multitrap using the transfer-matrix method which is generally applied for studying the energy spectrum of the unbounded quantum Kronig-Penney multibarrier. It was shown, by this method, that for certain values of the relevant parameters the bounded multitrap array have unity transmission and a double-peak phase transitional behaviour. We discuss in this work, using the same transfer matrix method, the energy related to the diffusion through the unbounded one-dimensional multitrap and find that it may be expressed in two entirely different ways with different results and consequences. Also, it is shown that, unlike the barriers in the Kronig-Penney case, the energies at one face of the imperfect trap greatly differ from the energies at the other face of the same trap.*

**keywords: Kronig-Penney system, Transfer matrix, Imperfect trap**

**Pacs numbers:** 71.15.Ap, 66.30.-h, 02.10.Yn

## 1 Introduction

The remarkable similarity [1, 2] between the Schroedinger and the classical diffusion equations have attracted many authors to discuss diffusion limited reactions using quantum methods and terminology (see annotated bibliography in [1]). For example, the same methods

and terminology of transfer matrices [3, 4, 5], which are applied [3, 4] for discussing quantum multibarrier potentials, have been used [6, 7] for discussing the one-dimensional bounded imperfect multitrapp system [8, 9, 10, 11] through which classical particles diffuse.

The imperfect trap, which was introduced in [12] and further discussed by others [13, 14, 15], may serve as a model for many physical situations. For example, one may find applications of it to rotational diffusion in chemical reactions [16] or to proteins with active sites deep inside the protein matrix [17] or to infinite lattice traversed by a random walker in the presence of an imperfect trap [13]. We note that the discussion of the *bounded* one-dimensional multitrapp systems have resulted, for certain values of its parameters [6, 7], in finding somewhat unconventional results. Among these one may count a unity transmission of the density of the diffusing particles through the multitrapp array [6] or the double-peak phase transition recently found [7] in such systems.

An important aspect of the classical one-dimensional multitrapp system which was not fully discussed thus far is when its length tends to infinity. The analogous quantum infinite multibarrier, which is the Kronig-Penney system [3, 4, 18], have been extensively discussed in the literature by many authors and it is known by its famous band-gap energy spectrum [3, 18] which is widely applied in electronics, semiconductors and solid state physics [19].

We discuss here the problem of a very large (infinite) one-dimensional multitrapp system using the same transfer matrix method which were applied for studying the Kronig-Penney multibarrier potential [3, 4, 18]. We, especially, discuss the energy of the diffusing particles and apply similar methods as those used for studying the energy spectrum of the quantum Kronig-Penney multibarrier [18, 19].

By using the transfer matrix method for the unbounded classical multitrapp system we obtain a quadratic characteristic equation the two solutions of which give rise to two possible expressions for the energy of the diffusing particles. Each of these two energies has a part

which is associated with the left hand face of the trap and another, differently expressed, part related to the right hand face of it. The different expressions of each of the two energies at the left and right hand sides of the trap causes these energies to greatly differ in value at these faces. That is, we show that by merely diffusing through the trap the particles's energy enormously changes. All the analytical results are graphically corroborated.

We note that the energies of the bounded one-dimensional multitrap system were found in [7] to have phase-transitional characteristics for the case in which an external field was appended to the system.

In Section II we apply the transfer matrix method for introducing and discussing the unbounded one-dimensional multitrap system as done in [6, 7]. Note that by using the transfer matrix formalism we also use its terminology which usually refers to an  $N$ -array system [4] rather than to an infinite array one. We remove this finiteness by letting the number of traps  $N$  and the total length  $L$  of the multitrap to become very large. In the numerical part we assign to  $N$  and  $L$  the values of 15000 and 20000 (note that in [4] a finite multi-barrier potential composed of a few hundred barriers was used as a model for the infinite Kronig-Penney system). In Section III we discuss the energy associated with the diffusing particles and find, using Appendices A and B, the appropriate expressions for it. In Section IV we calculate the energy for some specific values of its parameters. In Section V we use the analytical results of Sections III-IV and those of the Appendices A-B for graphically showing the energies as functions of its variables. We show that these variables have certain values at which the corresponding energy becomes disallowed such as, for example, when it tends to become negative or to assume very much large positive values. Some analytical expressions and derivations are shown in Appendices A-B. We conclude with a brief summary.

## 2 Application of the transfer matrix method for the unbounded one-dimensional multitrapping system

The one-dimensional imperfect multitrapping system is assumed to be arranged along the whole positive  $x$  axis and the diffusing particles which pass through it are supposed to come from the negative side of it. We denote, as in [6, 7], the total width of all the traps and the total interval among them by  $a$  and  $b$  respectively where  $a$  and  $b$  tend to become very much large. The ratio of  $b$  to  $a$  and the total length  $a + b$  of the system are denoted respectively by  $c$  and  $L$ . As in [6, 7] we may express  $a$  and  $b$  by  $c$  and  $L$  as  $a = \frac{L}{(1+c)}$ ,  $b = \frac{Lc}{(1+c)}$ . The period of the multibarrier system which is  $\frac{L}{N}$  is denoted by  $p$ . We assume that the multitrapping system begins at the point  $x = \frac{b}{N} = \frac{pc}{(1+c)}$ .

The initial and boundary value problem [20] which is appropriate for describing the diffusion through the  $N$  imperfect barriers is [6, 7]

$$\begin{aligned}
 1) \quad & \rho_t(x, t) = D\rho_{xx}(x, t), \quad t > 0, \quad 0 < x \leq (a + b) \\
 2) \quad & \rho(x, 0) = \rho_0 + f(x), \quad 0 < x \leq (a + b) \\
 3) \quad & \rho(x_i, t) = \frac{1}{k} \frac{d\rho(x, t)}{dx} \Big|_{x=x_i}, \quad t > 0, \quad 1 \leq i \leq 2N,
 \end{aligned} \tag{1}$$

where  $\rho(x, t)$ ,  $\rho_t(x, t)$  and  $\rho_{xx}(x, t)$  denote respectively the density of the diffusion particles, its first partial derivative with respect to the time  $t$  and its second partial derivative with respect to  $x$ . The diffusion constant  $D$  is supposed to have two different values;  $D_i$  inside the traps and  $D_e$  outside them where  $D_e > D_i$  [6, 7]. The value of  $0.5 \frac{cm^2}{sec}$  is the order of magnitude of the diffusion constant at room temperature and atmospheric pressure (P. 337 in [21]). In the numerical part here we have assigned to  $D_e$  and  $D_i$  the respective values of  $0.8 \frac{cm^2}{sec}$  and  $0.4 \frac{cm^2}{sec}$ . The second equation of the set (1) is the initial condition which is assumed [6, 7] to depend on  $x$  through  $f(x)$  and on the constant term  $\rho_0$ . The third equation

of the set (1) is the boundary value condition at the location of the traps where each trap has a finite width. That is, any trap is characterized by the two points along the  $x$  axis where its left and right hand faces are located. The constant  $k$  is the trapping rate (or the imperfection constant) which characterizes the degree of imperfection of the traps where the ideal trap condition is obtained when  $k \rightarrow \infty$ . The set (1) may be decomposed into two separate problems as follows [6, 7]

$$\begin{aligned}
1) \quad & \rho_t(x, t) = D\rho_{xx}, \quad t > 0, \quad 0 < x \leq (a + b) \\
2) \quad & \rho(x, 0) = \rho_0, \quad 0 < x \leq (a + b) \\
3) \quad & \rho(x_i, t) = \frac{1}{k} \frac{d\rho(x, t)}{dx} \Big|_{x=x_i}, \quad t > 0, \quad 1 \leq i \leq 2N
\end{aligned} \tag{2}$$

$$\begin{aligned}
1) \quad & \rho_t(x, t) = D\rho_{xx}(x, t), \quad t > 0, \quad 0 < x \leq (a + b) \\
2) \quad & \rho(x, 0) = f(x), \quad 0 < x \leq (a + b) \\
3) \quad & \rho(x_i, t) = 0, \quad t > 0, \quad 1 \leq i \leq 2N
\end{aligned} \tag{3}$$

The sets (2) and (3) respectively represent the diffusion through  $N$  imperfect and  $N$  ideal traps as may be realized from the third equations of these sets. Following [20] one may write the general solution of the set (1) as [6, 7]

$$\rho(x, t) = A\rho_1(x, t) + B\rho_2(x, t), \tag{4}$$

where  $\rho_1(x, t)$  and  $\rho_2(x, t)$  are respectively the solutions of the problems (2) and (3). Using

the method of separating variables [20] one may find the ideal trap solution [6, 7] as

$$\rho_2(x, t) = \sin\left(\frac{\pi x}{x_i}\right) e^{-\left(\frac{tD\pi^2}{x_i^2}\right)}, \quad 1 \leq i \leq 2N \quad (5)$$

The solution  $\rho_1(x, t)$  of the imperfect trap problem is given by [11]

$$\rho_1(x, t) = \rho_0\left(\operatorname{erf}\left(\frac{x - \dot{x}_i}{2\sqrt{Dt}}\right) + \exp(k^2Dt + k(x - \dot{x}_i))\operatorname{erfc}\left(k\sqrt{Dt} + \frac{(x - \dot{x}_i)}{2\sqrt{Dt}}\right)\right), \quad (6)$$

$$1 \leq i \leq 2N$$

where the  $\operatorname{erf}(x)$  and  $\operatorname{erfc}(x)$  are respectively the error and complementary error functions given by  $\operatorname{erf}(x) = \int_0^x e^{-u^2} du$  and  $\operatorname{erfc}(x) = 1 - \operatorname{erf}(x) = \int_x^\infty e^{-u^2} du$ . The  $\dot{x}_i$  denote the  $2N$  faces of the  $N$  traps. Using the transfer matrix method, as done in [3, 4] with respect to the Kronig-Penney potential and in [6, 7] with regard to the bounded multitrap system, one may write the following equation which relates the two faces of the  $j$ -th trap

$$\begin{pmatrix} A_{2j+1} \\ B_{2j+1} \end{pmatrix} = \begin{bmatrix} T_{11}(\dot{x}_j^{left}, \dot{x}_j^{right}) & T_{12}(\dot{x}_j^{left}, \dot{x}_j^{right}) \\ T_{21}(\dot{x}_j^{left}, \dot{x}_j^{right}) & T_{22}(\dot{x}_j^{left}, \dot{x}_j^{right}) \end{bmatrix} \begin{pmatrix} A_{2(j-1)+1} \\ B_{2(j-1)+1} \end{pmatrix}, \quad 1 \leq j \leq N \quad (7)$$

$A_{2j+1}$  and  $B_{2j+1}$  are respectively the imperfect and ideal trap coefficients respectively of the  $j$ -th trap and  $A_{2(j-1)+1}$  and  $B_{2(j-1)+1}$  are those of the  $(j - 1)$  trap. The two-dimensional matrix  $T^{(j)}$  at the right hand side of Eq (7) relates the left hand face of the  $j$ -th trap at  $\dot{x}_j^{left}$  to its right hand face at  $\dot{x}_j^{right}$  where  $\dot{x}_j^{right} > \dot{x}_j^{left}$ . The matrix elements  $T_{11}$ ,  $T_{12}$ ,  $T_{21}$  and  $T_{22}$  are derived in details in [6, 7] and are given in Appendix A.

For a one-dimensional  $N$  trap system, which begins at the point  $x = \frac{b}{N} = \frac{pc}{(1+c)}$  and has a period  $p$  one obtains the general transfer matrix equation [6, 7]

$$\begin{pmatrix} A_{2N+1} \\ B_{2N+1} \end{pmatrix} = T^{(N)}\left(p\left(N - \frac{1}{(1+c)}\right), pN\right) T^{(N-1)}\left(p\left(N - \frac{(2+c)}{(1+c)}\right), p(N-1)\right), \dots$$

$$\dots T^{(2)}\left(p\left(1 + \frac{c}{(1+c)}\right), 2p\right) T^{(1)}\left(\frac{pc}{(1+c)}, p\right) \begin{pmatrix} A_1 \\ B_1 \end{pmatrix} \quad (8)$$

Each two-dimensional matrix at the right hand side of the last equation is denoted in its parentheses by the locations of the left and right hand faces of its corresponding trap. Thus, one may realize, for example, that for an array which begins, as remarked, at the point  $x = \frac{b}{N} = \frac{pc}{(1+c)}$  the locations of the left and hand side faces of the  $N$ -th trap are  $x_N^{left} = p\left(N - \frac{1}{(1+c)}\right)$  and  $x_N^{right} = pN$  and those of the first trap are  $x_1^{left} = \frac{b}{N} = \frac{pc}{(1+c)}$  and  $x_1^{right} = \frac{a+b}{N} = p$ . Note that, as remarked in [6, 7], all the two-dimensional matrices at the right hand side of Eq (8) have the same values for  $D$ ,  $t$ ,  $L$  and  $c$  and differ by only the values of  $x$  along the positive spatial axis. Performing the  $N$  products at the right hand side of Eq (8) one may obtains an overall two-dimensional matrix, denoted  $\mathcal{T}_N$ , whose elements  $\mathcal{T}_{N11}$ ,  $\mathcal{T}_{N12}$ ,  $\mathcal{T}_{N21}$  and  $\mathcal{T}_{N22}$  may be recursively expressed by

$$\begin{aligned} \mathcal{T}_{N11} &= \mathcal{T}_{(N-1)11} T_{11}\left(p\left(N - \frac{1}{(1+c)}\right), Np\right) = \dots = \prod_{j=1}^{j=N} T_{11}\left(p\left(j - \frac{1}{(1+c)}\right), jp\right) \\ \mathcal{T}_{N12} &= \mathcal{T}_{(N-1)12} = \dots = \mathcal{T}_{212} = \mathcal{T}_{112} = T_{12} = 0 \\ \mathcal{T}_{N21} &= \mathcal{T}_{(N-1)21} T_{22}\left(p\left(N - \frac{1}{(1+c)}\right), Np\right) + \mathcal{T}_{(N-1)11} T_{21}\left(p\left(N - \frac{1}{(1+c)}\right), Np\right) \\ \mathcal{T}_{N22} &= \mathcal{T}_{(N-1)22} T_{22}\left(p\left(N - \frac{1}{(1+c)}\right), Np\right) = \dots = \prod_{j=1}^{j=N} T_{22}\left(p\left(j - \frac{1}{(1+c)}\right), jp\right) \end{aligned} \quad (9)$$

Note that whereas  $\mathcal{T}_{N11}$  and  $\mathcal{T}_{N22}$  are each a one-term expression which is constructed from  $N$  products the element  $\mathcal{T}_{N21}$  is an  $N$ -term expression each of them is composed of  $N$  products. Now, using Eq ( $A_2$ ) in Appendix A (see also the second of Eqs (9)) one may calculate the trace  $Tr$  and the determinant  $Det$  of the two-dimensional matrix  $T^{(j)}$  at the right hand side of Eq (7)

$$Tr(T^{(j)}) = T_{11}(\dot{x}_j^{left}, \dot{x}_j^{right}) + T_{22}(\dot{x}_j^{left}, \dot{x}_j^{right}) = T_{11}\left(p\left(j - \frac{1}{(1+c)}\right), pj\right) +$$

$$+T_{22}(p(j - \frac{1}{(1+c)}), pj) \quad (10)$$

$$\begin{aligned} Det(T^{(j)}) &= T_{11}(\dot{x}_j^{left}, \dot{x}_j^{right}) \cdot T_{22}(\dot{x}_j^{left}, \dot{x}_j^{right}) = T_{11}(p(j - \frac{1}{(1+c)}), pj) \cdot \\ &\cdot T_{22}(p(j - \frac{1}{(1+c)}), pj) \end{aligned}$$

Using Eqs (10), and following the analogous Kronig-Penney case [3, 4, 18], one may write the following quadratic characteristic equation of  $T^{(j)}$

$$\begin{aligned} y^2 - y \cdot Tr(T^{(j)}) + Det(T^{(j)}) &= y^2 - y \cdot (T_{11}(p(j - \frac{1}{(1+c)}), pj) + \\ &+ T_{22}(p(j - \frac{1}{(1+c)}), pj)) + T_{11}(p(j - \frac{1}{(1+c)}), pj) \cdot \\ &\cdot T_{22}(p(j - \frac{1}{(1+c)}), pj) = 0 \end{aligned} \quad (11)$$

The two roots  $y_+^{(j)}$  and  $y_-^{(j)}$  of the last equation which are the required eigenvalues of  $T^{(j)}$  are

$$y_+^{(j)} = T_{11}(p(j - \frac{1}{(1+c)}), pj), \quad y_-^{(j)} = T_{22}(p(j - \frac{1}{(1+c)}), pj) \quad (12)$$

Now, if the two roots  $y_+^{(j)}$ ,  $y_-^{(j)}$ ,  $1 \leq j \leq N$  are different as for the case here (see Eqs (A<sub>1</sub>) and (A<sub>4</sub>) in Appendix A), the two eigenvectors which correspond to them are linearly independent and we may identify, as for the corresponding quantum Kronig-Penney system

[3], the initial values  $\begin{pmatrix} A_1 \\ B_1 \end{pmatrix}$  from Eq (8) with the following two eigenvectors

$$\begin{aligned} T^{(1)} \begin{pmatrix} A_1^+ \\ B_1^+ \end{pmatrix} &= y_+^{(1)} \begin{pmatrix} A_1^+ \\ B_1^+ \end{pmatrix} = T_{11}(\frac{pc}{(1+c)}, p) \begin{pmatrix} A_1^+ \\ B_1^+ \end{pmatrix} \\ T^{(1)} \begin{pmatrix} A_1^- \\ B_1^- \end{pmatrix} &= y_-^{(1)} \begin{pmatrix} A_1^- \\ B_1^- \end{pmatrix} = T_{22}(\frac{pc}{(1+c)}, p) \begin{pmatrix} A_1^- \\ B_1^- \end{pmatrix}, \end{aligned} \quad (13)$$

where  $T^{(1)}$  at the left hand sides of Eqs (13) is the two-dimensional matrix from the right



hand side of Eq (7) for  $j = 1$  and  $\frac{pc}{(1+c)}$  and  $p$  at the right hand sides of Eqs (13) are, as mentioned, the respective locations of the left and right hand sides of the first trap. For these  $y_{\pm}^{(1)}$  one may identify, as for the Kronig-Penney case [3, 4], the coefficients  $\begin{pmatrix} A_{2N+1} \\ B_{2N+1} \end{pmatrix}$  in Eq (8) with the two eigenvectors

$$\begin{aligned} \begin{pmatrix} A_{2N+1}^+ \\ B_{2N+1}^+ \end{pmatrix} &= (y_+^{(1)})^N \begin{pmatrix} A_1^+ \\ B_1^+ \end{pmatrix} \\ \begin{pmatrix} A_{2N+1}^- \\ B_{2N+1}^- \end{pmatrix} &= (y_-^{(1)})^N \begin{pmatrix} A_1^- \\ B_1^- \end{pmatrix} \end{aligned} \quad (14)$$

From Eqs (A<sub>1</sub>), (A<sub>4</sub>), (A<sub>5</sub>) and (A<sub>7</sub>) in Appendix A and from realizing that the variables  $\dot{x}_i$  assume either the value of  $\dot{x}_j^{left}$  or  $\dot{x}_j^{right}$  (see, for example, the following discussion before Eq (31)) one may see that the quantities  $y_+^{(j)}$ ,  $1 \leq j \leq N$  are identical and satisfy  $y_+^{(1)} = y_+^{(2)} = \dots = y_+^{(N)}$ . The other quantities  $y_-^{(j)}$ ,  $1 \leq j \leq N$  can be seen to slightly differ from each other and one may approximately write  $y_-^{(1)} \approx y_-^{(2)} \approx \dots \approx y_-^{(N)}$ .

Considering the limit of an infinite multitrap array which is arranged along the whole positive  $x$  axis we should demand, as for the Kronig-Penney case [3, 4], that as the number of barriers  $N$  tend to  $\infty$  the right hand sides of Eqs (14) should not diverge. That is, we require

$$\begin{aligned} |y_+^{(1)}| &= \left| T_{11}\left(\frac{pc}{(1+c)}, p\right) \right| \leq 1 \\ |y_-^{(1)}| &= \left| T_{22}\left(\frac{pc}{(1+c)}, p\right) \right| \leq 1 \end{aligned} \quad (15)$$

Substituting in the last inequalities for  $T_{11}$  and  $T_{22}$  from Eqs (A<sub>1</sub>) and (A<sub>4</sub>) of Appendix A one obtains

$$\left| \frac{\alpha(D_e, \frac{pc}{(1+c)}, t)\alpha(D_i, p, t)}{\alpha(D_i, \frac{pc}{(1+c)}, t)\alpha(D_e, p, t)} \right| \leq 1 \quad (16)$$

$$\left| \frac{\eta(D_e, \frac{pc}{(1+c)}, t)\eta(D_i, p, t)}{\eta(D_i, \frac{pc}{(1+c)}, t)\eta(D_e, p, t)} \right| \leq 1, \quad (17)$$

where  $\alpha$  and  $\eta$  are given respectively by Eqs (A<sub>5</sub>) and (A<sub>7</sub>) in Appendix A.

### 3 The energy of the diffusing particles in the one-dimensional multitraps system

In order to be able to reduce the inequalities (16)-(17) to calculable expressions we express the parameters  $\alpha$  and  $\eta$ , which were given by Eqs (A<sub>5</sub>) and (A<sub>7</sub>) in Appendix A, in terms of the energy  $E$  of the diffusing particles. We use for that matter the relevant expressions of the energy which were fully derived and discussed in [7] for the multitraps system. Thus, using Eqs (4)-(6), we can write the energy  $E$  as

$$\begin{aligned} E(D, x, \dot{x}_i, t) &= \frac{1}{2}\rho v^2 = (\rho(D, x, \dot{x}_i, t))\frac{D}{t} = \left( A(x, D)\alpha(D, x, \dot{x}_i, t) + B(x, D)\rho_2(D, x, \dot{x}_i, t) \right) \cdot \\ \cdot \frac{D}{t} &= \left\{ A(x, D) \left( \operatorname{erf} \left( \frac{x - \dot{x}_i}{2\sqrt{Dt}} \right) + \exp(k^2 Dt + k(x - \dot{x}_i)) \operatorname{erfc} \left( k\sqrt{Dt} + \frac{x - \dot{x}_i}{2\sqrt{Dt}} \right) \right) + \right. \\ &+ B(x, D) \sin \left( \frac{\pi x}{\dot{x}_i} \right) \exp \left( -\frac{Dt\pi^2}{\dot{x}_i^2} \right) \left. \right\} \cdot \frac{D}{t}, \quad i = 1, 2, \dots, 2N, \quad t > 0, \end{aligned} \quad (18)$$

where  $v$  is the average diffusion velocity  $v = \sqrt{\frac{2D}{t}}$  which is derived from the classical one-dimensional diffusion equation for any finite  $t$  (see, for example P. 91 in [22]). The variables  $\dot{x}_i$  denote the locations on the  $x$  axis of the  $2N$  faces of the  $N$  traps (see the solutions (5)-(6) of the respective ideal and imperfect trap problems (3) and (2)). The imperfect and ideal trap coefficients  $A(x, D)$  and  $B(x, D)$  are numerically found for the  $2N$  faces of the  $N$  traps  $x = \dot{x}_j$ ,  $j = 1, 2, \dots, 2N$  [6, 7]. That is, for each  $j$ -th trap, one may find, using the transfer matrix method, the four pairs (1)  $A(\dot{x}_j^{left}, D_i), B(\dot{x}_j^{left}, D_i)$ , (2)  $A(\dot{x}_j^{right}, D_i), B(\dot{x}_j^{right}, D_i)$ , (3)  $A(\dot{x}_j^{left}, D_e), B(\dot{x}_j^{left}, D_e)$ , (4)  $A(\dot{x}_j^{right}, D_e), B(\dot{x}_j^{right}, D_e)$ . The first pair denotes the ideal

and imperfect trap coefficients *inside* the  $j$ -th trap at its left hand face. The second pair denotes these coefficients *inside* the  $j$ -th trap at its right hand face. The third and fourth pairs denote these coefficients *outside* the  $j$ -th trap at its left and right hand faces. Note that these coefficients, as well as the variables  $\hat{x}_j^{left}$  and  $\hat{x}_j^{right}$ , are not independent of each other. First, one may realize (see the discussion after Eq (8)) that  $\hat{x}_j^{left}$  and  $\hat{x}_j^{right}$  are given by  $\hat{x}_j^{left} = p(j - \frac{1}{(1+c)})$ ,  $\hat{x}_j^{right} = pj$ ,  $1 \leq j \leq N$  so that they are related by

$$\hat{x}_j^{left} = \hat{x}_j^{right} - \frac{p}{(1+c)}, \quad 1 \leq j \leq N \quad (19)$$

Second, the transfer matrix method relates the former coefficients of the  $j$ -th trap among themselves and also with those of the  $(j+1)$ -st trap as [6]

$$\begin{aligned} A(\hat{x}_j^{left}, D_i) &= A(\hat{x}_j^{right}, D_i), & A(\hat{x}_j^{right}, D_e) &= A(\hat{x}_{(j+1)}^{left}, D_e) \\ B(\hat{x}_j^{left}, D_i) &= B(\hat{x}_j^{right}, D_i), & B(\hat{x}_j^{right}, D_e) &= B(\hat{x}_{(j+1)}^{left}, D_e) \end{aligned} \quad (20)$$

As one may realize the  $\hat{x}_i$  from Eq (18) does not have to coincide with  $\hat{x}_j$ . That is, although for the same  $j$ -th trap each of  $\hat{x}_j$  and  $\hat{x}_i$  denote its two faces,  $\hat{x}_j$  may, for a specific context, refers to its left hand face in which case it is written as  $\hat{x}_j^{left}$  whereas  $\hat{x}_i$  may refers in this context to its right hand face and is written as  $\hat{x}_j^{right}$ .

Now, analogously to the Kronig-Penney case [3, 4, 18], one may turn the inequalities at the right hand sides of (16)-(17) to equalities. In such case the left hand sides of (16)-(17) are equated to  $\cos(\kappa p)$  where  $\kappa$  is a real parameter and  $p$  is the period of the multitraps which is  $p = \frac{L}{N}$ . In accordance with the analogous procedure of the Kronig-Penney case [3, 4, 18] the two eigenvalues of the characteristic equation are related to the same parameter. Note that even if one relates the two eigenvalues to different parameters he will obtain the same following expressions (31)-(34) for the energies each of which depends on only one parameter.

We use in the following the transfer matrix principal property in which the density (and its derivative) at the two sides of any face of each trap are equal [3, 4, 6]. This may be expressed, for example, for the left hand face of the  $j$ -th trap as

$$\begin{aligned} \rho(D_e, \dot{x}_j^{left}, \dot{x}_i, t) &= A(\dot{x}_j^{left}, D_e)\alpha(D_e, \dot{x}_j^{left}, \dot{x}_i, t) + B(\dot{x}_j^{left}, D_e)\rho_2(D_e, \dot{x}_j^{left}, \dot{x}_i, t) = \\ &= \rho(D_i, \dot{x}_j^{left}, \dot{x}_i, t) = A(\dot{x}_j^{left}, D_i)\alpha(D_i, \dot{x}_j^{left}, \dot{x}_i, t) + B(\dot{x}_j^{left}, D_i)\rho_2(D_i, \dot{x}_j^{left}, \dot{x}_i, t) \end{aligned} \quad (21)$$

Substituting from Eq (18) for the  $\alpha$ 's in (16) and from Eqs (5), (18) and (A<sub>7</sub>) for the  $\eta$ 's in (17) one obtains after equating the left hand sides of (16)-(17) to  $\cos(\kappa p)$  (see the discussion after Eq (20))

$$\begin{aligned} &\frac{\left(\frac{E(D_e, \frac{pc}{(1+c)}, \dot{x}_i, t)t}{A(\frac{pc}{(1+c)}, D_e)D_e} - \frac{B(\frac{pc}{(1+c)}, D_e)\rho_2(D_e, \frac{pc}{(1+c)}, \dot{x}_i, t)}{A(\frac{pc}{(1+c)}, D_e)}\right) \cdot \left(\frac{E(D_i, p, \dot{x}_i, t)t}{A(p, D_i)D_i} - \frac{B(p, D_i)\rho_2(D_i, p, \dot{x}_i, t)}{A(p, D_i)}\right)}{\left(\frac{E(D_i, \frac{pc}{(1+c)}, \dot{x}_i, t)t}{A(\frac{pc}{(1+c)}, D_i)D_i} - \frac{B(\frac{pc}{(1+c)}, D_i)\rho_2(D_i, \frac{pc}{(1+c)}, \dot{x}_i, t)}{A(\frac{pc}{(1+c)}, D_i)}\right) \cdot \left(\frac{E(D_e, p, \dot{x}_i, t)t}{A(p, D_e)D_e} - \frac{B(p, D_e)\rho_2(D_e, p, \dot{x}_i, t)}{A(p, D_e)}\right)} = \\ &= \cos(\kappa p) \end{aligned} \quad (22)$$

$$\begin{aligned} &\frac{\left(\frac{E(D_e, \frac{pc}{(1+c)}, \dot{x}_i, t)t}{B(\frac{pc}{(1+c)}, D_e)D_e} - \frac{A(\frac{pc}{(1+c)}, D_e)\alpha(D_e, \frac{pc}{(1+c)}, \dot{x}_i, t)}{B(\frac{pc}{(1+c)}, D_e)}\right) \cdot \left(\frac{E(D_i, p, \dot{x}_i, t)t}{B(p, D_i)D_i} - \frac{A(p, D_i)\alpha(D_i, p, \dot{x}_i, t)}{B(p, D_i)}\right)}{\left(\frac{E(D_i, \frac{pc}{(1+c)}, \dot{x}_i, t)t}{B(\frac{pc}{(1+c)}, D_i)D_i} - \frac{A(\frac{pc}{(1+c)}, D_i)\alpha(D_i, \frac{pc}{(1+c)}, \dot{x}_i, t)}{B(\frac{pc}{(1+c)}, D_i)}\right) \cdot \left(\frac{E(D_e, p, \dot{x}_i, t)t}{B(p, D_e)D_e} - \frac{A(p, D_e)\alpha(D_e, p, \dot{x}_i, t)}{B(p, D_e)}\right)} = \\ &= \cos(\kappa p) \end{aligned} \quad (23)$$

The functions  $\rho_2$  and  $\alpha$  are given respectively by Eqs (5) and (A<sub>5</sub>) in Appendix A and use is made of the relation  $\rho_2(D, x, \dot{x}_i, t) = -\frac{\dot{x}_i}{\pi}\eta(D, \dot{x}_i, t) \sin(\frac{\pi x}{\dot{x}_i})$  obtained by comparing Eq (5) with Eq (A<sub>7</sub>) in Appendix A. The sine function and the factor  $\frac{\dot{x}_i}{\pi}$  which do not depend on the diffusion constants  $D_i$  and  $D_e$  are cancelled in Eq (23). As realized from the last equations there are four energies related to the trap;  $E(D_e, \frac{pc}{(1+c)}, \dot{x}_i, t)$ ,  $E(D_e, p, \dot{x}_i, t)$ ,  $E(D_i, \frac{pc}{(1+c)}, \dot{x}_i, t)$ , and  $E(D_i, p, \dot{x}_i, t)$ . But, as seen, one may reduce the number of the energies related to each trap to two since using Eqs (18) and (21) one may obtain the following expressions which

relate the energies at the two sides of each trap

$$\begin{aligned}
E(D_e, \dot{x}_j^{left}, \dot{x}_i, t) \frac{t}{D_e} &= E(D_i, \dot{x}_j^{left}, \dot{x}_i, t) \frac{t}{D_i}, \quad 1 \leq j \leq N \\
E(D_e, \dot{x}_j^{right}, \dot{x}_i, t) \frac{t}{D_e} &= E(D_i, \dot{x}_j^{right}, \dot{x}_i, t) \frac{t}{D_i}, \quad 1 \leq j \leq N
\end{aligned} \tag{24}$$

In the following we use Eqs (22)-(24) for finding the two energies  $E(D_e, p, \dot{x}_i, t)$  and  $E(D_e, \frac{pc}{(1+c)}, \dot{x}_i, t)$  which are respectively the energies at the right and left hand faces of the trap. Thus, using Eqs (24) we may rewrite Eqs (22)-(23) as follows

$$\begin{aligned}
&\frac{(E(D_e, \frac{pc}{(1+c)}, \dot{x}_i, t) t - D_e B(\frac{pc}{(1+c)}, D_e) \rho_2(D_e, \frac{pc}{(1+c)}, \dot{x}_i, t)) \cdot (E(D_e, p, \dot{x}_i, t) t - D_e B(p, D_e) \rho_2(D_i, p, \dot{x}_i, t))}{(E(D_e, \frac{pc}{(1+c)}, \dot{x}_i, t) t - D_e B(\frac{pc}{(1+c)}, D_i) \rho_2(D_i, \frac{pc}{(1+c)}, \dot{x}_i, t)) \cdot (E(D_e, p, \dot{x}_i, t) t - D_e B(p, D_e) \rho_2(D_e, p, \dot{x}_i, t))} = \\
&= \frac{A(\frac{pc}{(1+c)}, D_e)}{A(p, D_e)} \cos(\kappa p)
\end{aligned} \tag{25}$$

$$\begin{aligned}
&\frac{(E(D_e, \frac{pc}{(1+c)}, \dot{x}_i, t) t - D_e A(\frac{pc}{(1+c)}, D_e) \alpha(D_e, \frac{pc}{(1+c)}, \dot{x}_i, t)) \cdot (E(D_e, p, \dot{x}_i, t) t - D_e A(p, D_e) \alpha(D_i, p, \dot{x}_i, t))}{(E(D_e, \frac{pc}{(1+c)}, \dot{x}_i, t) t - D_e A(\frac{pc}{(1+c)}, D_i) \alpha(D_i, \frac{pc}{(1+c)}, \dot{x}_i, t)) \cdot (E(D_e, p, \dot{x}_i, t) t - D_e A(p, D_e) \alpha(D_e, p, \dot{x}_i, t))} = \\
&= \frac{B(\frac{pc}{(1+c)}, D_e)}{B(p, D_e)} \cos(\kappa p)
\end{aligned} \tag{26}$$

The two quadratic equations (25)-(26) were simultaneously solved in Appendix B for the energies  $E(D_e, p, \dot{x}_i, t)$  and  $E(D_e, \frac{pc}{(1+c)}, \dot{x}_i, t)$  and two separate solutions were found for each (see Eqs (B<sub>6</sub>)-(B<sub>9</sub>) in Appendix B). For  $E(D_e, p, \dot{x}_i, t)$  we find the two solutions of

$$E^+(D_e, p, \dot{x}_i, t) = \frac{t(X_1 X_4 - X_5) Y_3 - (X_1 X_2 X_4 - X_3 X_5) Y_1}{(t X_3 - t X_1 X_2) Y_1 - t^2 (1 - X_1) Y_3} \tag{27}$$

$$E^-(D_e, p, \dot{x}_i, t) = \frac{Y_2}{Y_1} \tag{28}$$

And for  $E(D_e, \frac{pc}{(1+c)}, \dot{x}_i, t)$  we find the two solutions of

$$E^+(D_e, \frac{pc}{(1+c)}, \dot{x}_i, t) = \frac{Y_3}{Y_1} \quad (29)$$

$$E^-(D_e, \frac{pc}{(1+c)}, \dot{x}_i, t) = \quad (30)$$

$$= \frac{(X_3 - X_1 X_2)((tX_3 - tX_1 X_2)Y_2 + (X_1 X_2 X_4 - X_3 X_5)Y_1) - (1 - X_1)(t^2(X_3 - X_1 X_2)(Y_4 - Y_5) + t(X_1 X_2 X_4 - X_3 X_5)Y_3)}{(X_3 - X_1 X_2)((t^2(1 - X_1)Y_2 + t(X_1 X_4 - X_5)Y_1) - (1 - X_1)(t^3(1 - X_1)(Y_4 - Y_5) + t^2(X_1 X_4 - X_5)Y_3))},$$

where the quantities  $X_1, X_2, X_3, X_4, X_5$  and  $Y_1, Y_2, Y_3, Y_4, Y_5$  are given respectively by Eqs (B<sub>1</sub>) and (B<sub>4</sub>) in Appendix B. The energies  $E^+(D_e, p, \dot{x}_i, t)$  and  $E^-(D_e, p, \dot{x}_i, t)$  from Eqs (27)-(28) are for the right hand side of the trap and the energies  $E^+(D_e, \frac{pc}{(1+c)}, \dot{x}_i, t)$  and  $E^-(D_e, \frac{pc}{(1+c)}, \dot{x}_i, t)$  from Eqs (29)-(30) are for the left hand side of it.

In the former expressions of the energies the variable  $\dot{x}_i$  must coincides with either  $\frac{pc}{(1+c)}$  or  $p$ . Thus, when  $\dot{x}_i = \frac{pc}{(1+c)}$  one have to discard the solutions  $E^-(D_e, \frac{pc}{(1+c)}, \frac{pc}{(1+c)}, t)$  and  $E^-(D_e, p, \frac{pc}{(1+c)}, t)$  since in this case one obtains from Eq (5) and from Eqs (B<sub>1</sub>) in Appendix B  $X_2 = X_3 = 0$ . In this case the energy  $E^-(D_e, \frac{pc}{(1+c)}, \frac{pc}{(1+c)}, t)$  from Eq (30) vanishes whereas the energy  $E^-(D_e, p, \frac{pc}{(1+c)}, t)$  from Eq (28) remains at the value of  $\frac{Y_2}{Y_1}$ . This implied the unreasonable conclusion that the passing particles have no energies at the left hand face of the trap before they diffuse through it whereas at the right hand face of it they have non-vanishing unaccountable energies. Thus, for  $\dot{x}_i = \frac{pc}{(1+c)}$  only the energies  $E^+(D_e, p, \frac{pc}{(1+c)}, t)$  and  $E^+(D_e, \frac{pc}{(1+c)}, \frac{pc}{(1+c)}, t)$  must be considered and they are given by

$$E^+(D_e, p, \frac{pc}{(1+c)}, t) = \frac{(X_1 X_4 - X_5)}{t(X_1 - 1)} \quad (31)$$

$$E^+(D_e, \frac{pc}{(1+c)}, \frac{pc}{(1+c)}, t) = \frac{Y_3}{Y_1} \quad (32)$$

The second case is that of  $\dot{x}_i = p$  for which one obtains from Eq (5) and from Eqs (B<sub>1</sub>) in Appendix B  $X_4 = X_5 = 0$ . In this case the energy  $E^+(D_e, p, p, t)$  from Eq (27) vanishes

whereas the energy  $E^+(D_e, \frac{pc}{(1+c)}, p, t)$  from Eq (29) remains in the value of  $\frac{Y_3}{Y_1}$ . This also could not be accepted since it implied that the particles suddenly stop diffusing after the first trap whereas we are concerned with the diffusion along the entire multitraps system. Thus, the energies  $E^+(D_e, p, p, t)$  and  $E^+(D_e, \frac{pc}{(1+c)}, p, t)$  must be discarded and we have to take into account only the energies  $E^-(D_e, p, p, t)$  and  $E^-(D_e, \frac{pc}{(1+c)}, p, t)$  which are given by

$$E^-(D_e, \frac{pc}{(1+c)}, p, t) = \frac{(X_3 - X_1 X_2)}{t(1 - X_1)} \quad (33)$$

$$E^-(D_e, p, p, t) = \frac{Y_2}{Y_1} \quad (34)$$

If  $c$  becomes very large so that  $c \gg 1$  one may realize from Eqs ( $B_1$ ) in Appendix B and Eqs (5), (31) and (33) that the energies  $E^+(D_e, p, \frac{pc}{(1+c)}, t)$  and  $E^-(D_e, \frac{pc}{(1+c)}, p, t)$  tend to zero.

## 4 Calculation of the energies (31)-(34) for specific values of $\kappa p$ .

The expressions (31)-(34) for the energies  $E^+(D_e, p, \frac{pc}{(1+c)}, t)$ ,  $E^+(D_e, \frac{pc}{(1+c)}, \frac{pc}{(1+c)}, t)$ ,  $E^-(D_e, \frac{pc}{(1+c)}, p, t)$ ,  $E^-(D_e, p, p, t)$  should now be evaluated as functions of  $\kappa p$  as done for the quantum Kronig-Penney system [3, 4, 18]. But before doing that we show that the expressions (31)-(34) become simplified for certain values of  $\kappa p$ . Thus, for  $\kappa p = \frac{\pi}{2} + n\pi$ ,  $n = 0, 1, 2, \dots$  one have  $\cos(\kappa p) = 0$  and from Eqs ( $B_4$ ) and the first of Eqs ( $B_1$ ) in Appendix B we have  $Y_5 = X_1 = 0$  and also the second terms of  $Y_1$ ,  $Y_2$  and  $Y_3$  vanish as well. Thus, the energies (31)-(34) become

$$E^+_{(\cos(\kappa p)=0)}(D_e, p, \frac{pc}{(1+c)}, t) = \frac{X_5}{t} = \frac{D_e B(p, D_i) \rho_2(D_i, p, \frac{pc}{(1+c)}, t)}{t} \quad (35)$$

$$E_{(\cos(\kappa p)=0)}^+(D_e, \frac{pc}{(1+c)}, \frac{pc}{(1+c)}, t) = \frac{D_e A(\frac{pc}{(1+c)}, D_e) \alpha(D_e, \frac{pc}{(1+c)}, \frac{pc}{(1+c)}, t)}{t} = \frac{D_e A(\frac{pc}{(1+c)}, D_e)}{t} \cdot \exp(k^2 D_e t) \operatorname{erfc}(k \sqrt{D_e t}) \quad (36)$$

$$E_{(\cos(\kappa p)=0)}^-(D_e, \frac{pc}{(1+c)}, p, t) = \frac{X_3}{t} = \frac{D_e B(\frac{pc}{(1+c)}, D_e) \rho_2(D_e, \frac{pc}{(1+c)}, p, t)}{t} \quad (37)$$

$$E_{(\cos(\kappa p)=0)}^-(D_e, p, p, t) = \frac{D_e A(p, D_i) \alpha(D_i, p, p, t)}{t} = \frac{D_e A(p, D_i)}{t} \cdot \exp(k^2 D_i t) \operatorname{erfc}(k \sqrt{D_i t}) \quad (38)$$

For obtaining Eqs (35) and (37) we respectively use the fifth and third of Eqs ( $B_1$ ) in Appendix B and for Eqs (36) and (38) we respectively use the third and second of Eqs ( $B_4$ ) in Appendix B. Use is also made of Eq ( $A_5$ ) in Appendix A and the first of Eqs ( $B_4$ ) in Appendix B.

Another kind of points which draw special attention is  $\kappa p = \arccos(\frac{A(p, D_e)}{A(\frac{pc}{(1+c)}, D_e)})$  for which one obtains from the first of Eqs ( $B_1$ ) in Appendix B  $X_1 = 1$ . At these points the energies  $E^+(D_e, p, \frac{pc}{(1+c)}, t)$  and  $E^-(D_e, \frac{pc}{(1+c)}, p, t)$  from Eqs (31) and (33) must be discarded since they tend to infinity and this can not be accepted on physical grounds. Note that using the transfer matrix method one may conclude that the ideal traps coefficients always satisfy  $B(\dot{x}_j^{\text{right}}, D_e) > B(\dot{x}_j^{\text{left}}, D_e)$  and so the division  $\frac{B(p, D_e)}{B(\frac{pc}{(1+c)}, D_e)}$  is greater than unity which implies that the quantity  $Y_1$ , as defined by the first of Eqs ( $B_4$ ) in Appendix B, is always positive. This determines, as will be shown, the values and the graphical form of the energies  $E^+(D_e, \frac{pc}{(1+c)}, \frac{pc}{(1+c)}, t)$  and  $E^-(D_e, p, p, t)$  from Eqs (32) and (34).



## 5 The energies as functions of $\kappa p$ , $c$ , $k$ , and $t$ .

As seen from Eqs ( $B_1$ ) and ( $B_4$ ) in Appendix B, ( $A_5$ ) in Appendix A and from Eqs (5)-(6) the energies (31)-(34) critically depend upon the ratio  $c$ , the trapping rate  $k$  and the time  $t$ . Also, one may conclude from the analytical form of the expressions (31)-(34) and from the Panels of Figures 1-4 that the energy  $E^+(D_e, p, \frac{pc}{(1+c)}, t)$  from Eq (31) corresponds to  $E^-(D_e, \frac{pc}{(1+c)}, p, t)$  from Eq (33) and  $E^+(D_e, \frac{pc}{(1+c)}, \frac{pc}{(1+c)}, t)$  from Eq (32) corresponds to  $E^-(D_e, p, p, t)$  from Eq (34). That is,  $E^+(D_e, p, \frac{pc}{(1+c)}, t)$  and  $E^-(D_e, \frac{pc}{(1+c)}, p, t)$  are expressed only by the ideal trap expressions from Eqs ( $B_1$ ) in Appendix B and  $E^+(D_e, \frac{pc}{(1+c)}, \frac{pc}{(1+c)}, t)$  and  $E^-(D_e, p, p, t)$  are given only by the imperfect trap expressions from Eqs ( $B_4$ ) of Appendix B. The corresponding energies  $E^+(D_e, p, \frac{pc}{(1+c)}, t)$  and  $E^-(D_e, \frac{pc}{(1+c)}, p, t)$  as functions of  $\kappa p$  are characterized with a behaviour which causes them to abruptly change their values in a rather jumpy and discontinuous way (see, for example, the Panels of Figures 1-2). As one may assume these abrupt changes in the energies (31) and (33) are related to the values of  $\kappa p$  for which ( $X_1$ ) in their denominator is close to 1. Note that the nonzero values of these energies may be negative in which case they can not represent real energies since we discuss here only kinetic energies as realized from Eq (18). The second corresponding pair of energies  $E^+(D_e, \frac{pc}{(1+c)}, \frac{pc}{(1+c)}, t)$  and  $E^-(D_e, p, p, t)$  are characterized as steeply increasing with  $\kappa p$  for very small values of it and at  $\kappa p \approx 0.05$  they become constant (as functions of  $\kappa p$ ) for all  $\kappa p > 0.05$  (see, for example, the Panels of Figures 3 and 4). Also, in contrast to the former pair, these energies are always positive.

From the Panels of Figures 1-4 one may realize that, for the same values of  $c$ ,  $k$  and  $t$ , the nonzero values of the energy  $E^-(D_e, \frac{pc}{(1+c)}, p, t)$  are generally greater by several orders of magnitude from the other three energies (see, for example, Panels 1-2 of Figure 4 which show a giant difference of  $10^{44}$  between  $E^-(D_e, \frac{pc}{(1+c)}, p, t)$  and  $E^+(D_e, p, \frac{pc}{(1+c)}, t)$ ). Thus, although, as mentioned, the energies  $E^-(D_e, p, p, t)$  and  $E^-(D_e, \frac{pc}{(1+c)}, p, t)$  correspond in analytical expres-

sions and graphical form as functions of  $\kappa p$  to the respective energies  $E^+(D_e, \frac{pc}{(1+c)}, \frac{pc}{(1+c)}, t)$  and  $E^+(D_e, p, \frac{pc}{(1+c)}, t)$  they greatly differ in value. This may be seen from Panels 1 and 2 of Figure 1 which, respectively, show the energies  $E^-(D_e, \frac{pc}{(1+c)}, p, t)$  and  $E^+(D_e, p, \frac{pc}{(1+c)}, t)$  as functions of  $\kappa p$  using the same 20 different values of the ratio  $c$  for each Panel and the same  $t$  and  $k$  for all the graphs shown. The 20 values of  $c$  are  $c = 0.1 + n \cdot 0.4$ ,  $n = 0, 1, 2, \dots, 19$  and the values of  $t$  and  $k$  for all the graphs shown in the two Panels are  $t = k = 2$ . Note that although the energies shown in Panels 1 and 2 look similar as functions of  $\kappa p$  the nonzero values of these energies differ by as much as  $10^4$ . As mentioned, we should consider only the zero or the positive parts of the graphs as representing real kinetic energy.

In Panels 3 and 4 of Figure 1 we show enlarged views of the small sections in the respective Panels 1 and 2 just to the right of the point  $\kappa p = 0$ . Note the similarity between these energies even at this small resolution and also note that despite this similarity the nonzero parts of the energy in Panel 3 are about  $0.5 \cdot 10^4 \text{ erg}$  whereas those of Panel 4 are about  $0.4 \text{ erg}$ . The largest hooked negative graph corresponds to the smallest value of  $c$  and as  $c$  increases the other hooked positive and negative graphs are added. The larger  $c$  becomes in Panels 3-4 the corresponding energies become smaller and tend to be densely arrayed around zero. This means that the larger is the interval between the traps compared to their width the kinetic energy of the diffusing particles tends to decrease to zero.

The same similarity in graphical form and same large differences in values may be shown for the same energies from Figure 1, as functions of  $\kappa p$ , but now for different values of the trapping rate  $k$ . This is seen in Panels 1 and 2 of Figure 2 which respectively show the energies  $E^-(D_e, \frac{pc}{(1+c)}, p, t)$  and  $E^+(D_e, p, \frac{pc}{(1+c)}, t)$  as functions of  $\kappa p$  using the same 20 different values of  $k$  for each Panel and the same  $t$  and  $c$  for all the graphs shown. The 20 values of  $k$  for each panel are  $k = 0.1 + n \cdot 0.4$ ,  $n = 1, 2, \dots, 19$  and the values of  $t$  and  $c$  for all the graphs in the two Panels are  $t = 2$  and  $c = 1$ . As for Panels 1 and 2 of Figure 1 the differences between the nonzero parts of these energies amount to about  $10^4$  although they

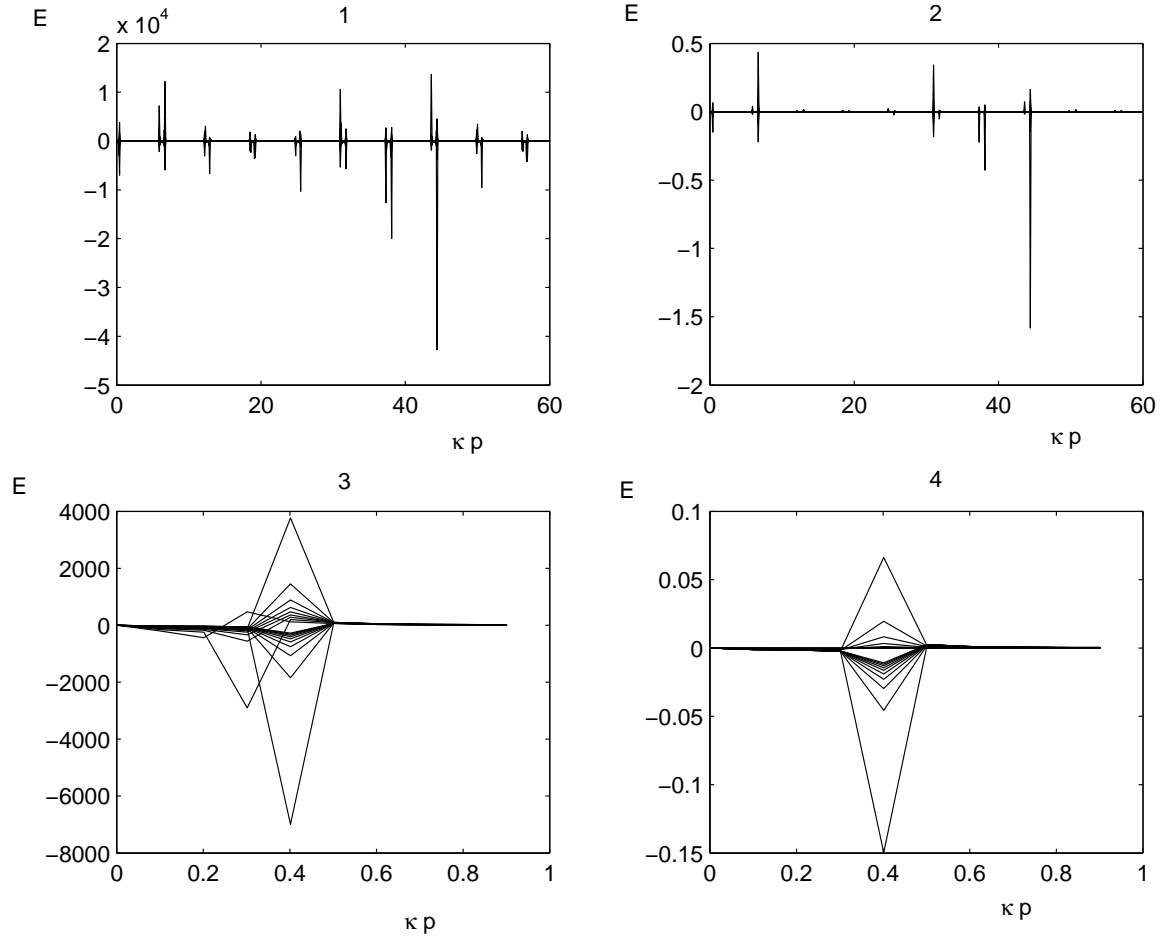


Figure 1: Panels 1 and 2 respectively show the energies  $E^-(D_e, \frac{pc}{(1+c)}, p, t)$  and  $E^+(D_e, p, \frac{pc}{(1+c)}, t)$  as functions of  $\kappa p$  for the 20 values of the ratio  $c = 0.1 + n \cdot 0.4$ ,  $n = 0, 1, 2, \dots, 19$ . Panels 3 and 4 show a high resolution of the respective neighbourhoods in Panels 1 and 2 just to the right of the point  $\kappa p = 0$ . Note that although Panels 1 and 2 as well as Panels 3 and 4 are similar in form they greatly differ in the nonzero values of their energies. Both the trapping rate  $k$  and the time  $t$  have the values of  $k = t = 2$  for all the graphs of the four Panels. The units of the energies are in *ergs*.

look similar in external form. Note that actually the energy in Panel 2 tends to zero. Panels 3 and 4 of Figure 2 respectively show enlarged views of the respective neighbourhoods from Panels 1 and 2 about the point  $\kappa p = 25$ . One may note the similarity between these energies even at this small resolution. Also, one may note that despite this apparent similarity the nonzero parts of the energy in Panel 3 is about  $10^4$  whereas the corresponding ones in Panel 4 tend to zero.

For both Panels 3 and 4 the graphs with the large dense hooked positive parts correspond to the smallest values of  $k$  which means, as one may assume, that the smaller is the trapping rate of the traps the larger is the energy of the diffusing particles. As  $k$  increases the corresponding graphs become negative and they tend to zero for large enough  $k$ . That is, the more  $k$  grows which means that the larger becomes the trapping rate of the trap the more restrained and blocked become the diffusing particles in their passage through it. This is demonstrated through the vanishing of the positive allowed parts of the energies for large  $k$  and their tendency to the zero value.

In the Panels of Figures 1-2 we compare for different values of  $c$  and  $k$  the two corresponding energies  $E^-(D_e, \frac{pc}{(1+c)}, p, t)$  and  $E^+(D_e, p, \frac{pc}{(1+c)}, t)$  as functions of  $\kappa p$ . We now discuss the second pair of corresponding energies  $E^-(D_e, p, p, t)$  and  $E^+(D_e, \frac{pc}{(1+c)}, \frac{pc}{(1+c)}, t)$ . Compared to the energies  $E^-(D_e, \frac{pc}{(1+c)}, p, t)$  and  $E^+(D_e, p, \frac{pc}{(1+c)}, t)$  from Figures 1-2 the energies  $E^-(D_e, p, p, t)$  and  $E^+(D_e, \frac{pc}{(1+c)}, \frac{pc}{(1+c)}, t)$  are always positive and they are generally constant with  $\kappa p$ . Panels 1 and 2 respectively show three-dimensional surfaces of the energies  $E^-(D_e, p, p, t)$  and  $E^+(D_e, \frac{pc}{(1+c)}, \frac{pc}{(1+c)}, t)$  as functions of  $\kappa p$  and  $c$  and for the values of  $k = t = 2$ . Note that the energy  $E^+(D_e, \frac{pc}{(1+c)}, \frac{pc}{(1+c)}, t)$  at Panel 2 does not depend at all on either  $\kappa p$  or  $c$  and has the rather small constant value of 0.088 *erg*. The energy  $E^-(D_e, p, p, t)$  at Panel 1 is constant for all  $\kappa p$ 's and depends only slightly on  $c$  as seen from the small depression of the surface at small  $c$  which causes it to be slightly distorted from the planar form of Panel 2. Panels 3 and 4 respectively show three-dimensional surfaces of the same energies from Panels 1 and

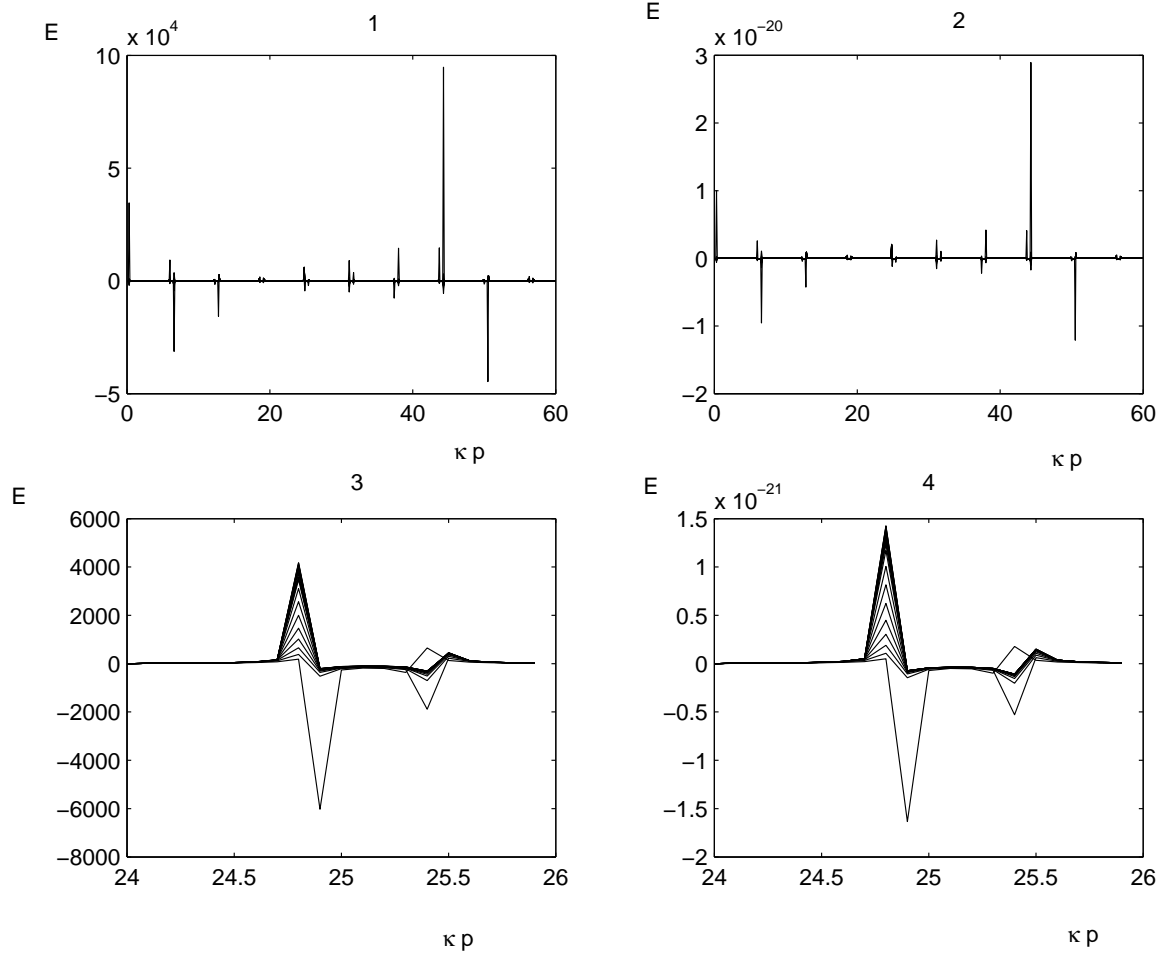


Figure 2: Panels 1 and 2 respectively show the energies  $E^-(D_e, \frac{pc}{(1+c)}, p, t)$  and  $E^+(D_e, p, \frac{pc}{(1+c)}, t)$  as functions of  $\kappa p$  for the 20 values of the trapping rate  $k = 0.1 + n \cdot 0.4$ ,  $n = 0, 1, 2, \dots, 19$ . Panel 3 and 4 show a high resolution of the respective neighbourhoods in Panels 1 and 2 of the point  $\kappa p = 25$ . As is the case for the Panels of Figure 1 one may note that although Panels 1 and 2 as well as Panels 3 and 4 are very similar in form nevertheless they greatly differ in the nonzero values of their energies. The ratio  $c$  and the time  $t$  have the respective values of  $c = 1$  and  $t = 2$  for all the graphs of the four Panels. The energies are in units of *ergs*.

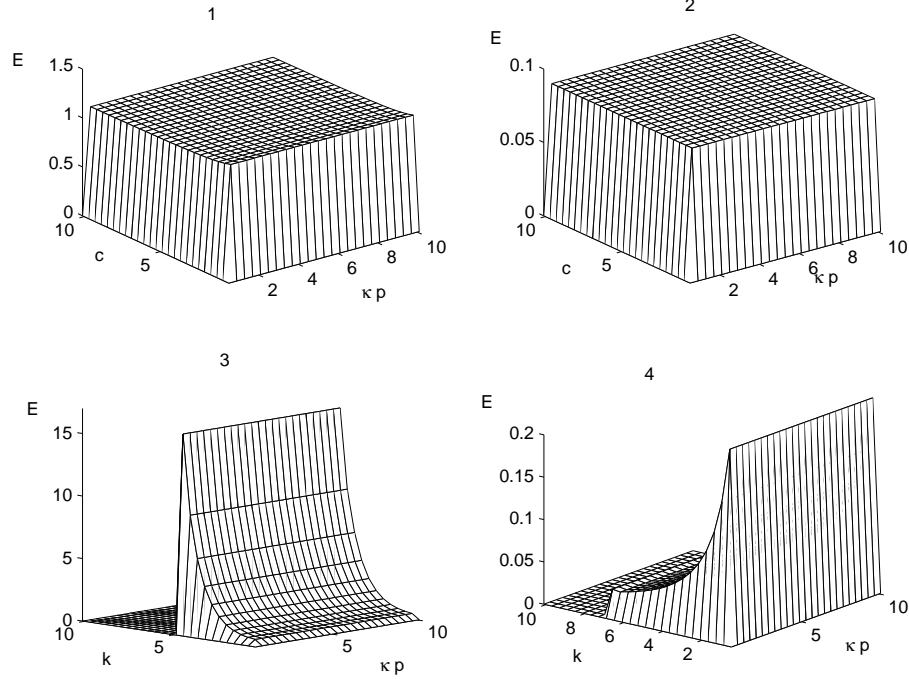


Figure 3: Panels 1 and 2 respectively show three-dimensional surfaces of the energies  $E^-(D_e, p, p, t)$  and  $E^+(D_e, \frac{pc}{(1+c)}, \frac{pc}{(1+c)}, t)$  as functions of  $\kappa p$  and  $c$  and for  $k = t = 2$ . Note that the energy  $E^+(D_e, \frac{pc}{(1+c)}, \frac{pc}{(1+c)}, t)$  at Panel 2 does not depend on either  $\kappa p$  or  $c$  and has the constant value of  $0.088 \text{ erg}$ . The energy  $E^+(D_e, p, p, t)$  at Panel 1 depends only slightly on  $c$ , is constant for all  $\kappa p$ 's and have a maximum value (for  $k = 2$ ) of  $E_{max}^+(D_e, p, p, t) = 1 \text{ erg}$ . Panels 3 and 4 respectively show three-dimensional surfaces of the same energies from Panels 1 and 2 but now as functions of  $\kappa p$  and  $k$  and for  $c = 1$  and  $t = 2$ . Note that these energies do not depend at all on  $\kappa p$  and vary with  $k$  to the maxima (for  $c = 1$ ) of  $E_{max}^-(D_e, p, p, t) = 15 \text{ erg}$  and  $E_{max}^+(D_e, \frac{pc}{(1+c)}, \frac{pc}{(1+c)}, t) = 0.23 \text{ erg}$ . Note also that the energies  $E^-(D_e, p, p, t)$  and  $E^+(D_e, \frac{pc}{(1+c)}, \frac{pc}{(1+c)}, t)$  drop respectively to zero at  $k \approx 4.8$  and  $k \approx 6.3$ .

2 but now as functions of  $\kappa p$  and  $k$  and for the values  $c = 1$  and  $t = 2$ . Note that these energies, as in Panels 1 and 2, do not depend on  $\kappa p$  and vary with  $k$  to the maxima (for  $c = 1$ ) of  $E_{max}^-(D_e, p, p, t) = 15 \text{ erg}$  and  $E_{max}^+(D_e, \frac{pc}{(1+c)}, \frac{pc}{(1+c)}, t) = 0.23 \text{ erg}$ . Note also that as the trapping rate  $k$  grows the energies  $E^-(D_e, p, p, t)$  and  $E^+(D_e, \frac{pc}{(1+c)}, \frac{pc}{(1+c)}, t)$  decrease in value and become zero at the respective values of  $k \approx 4.8$  and  $k \approx 6.3$ . This result is expected since as the trapping rate grows the traps become more effective in blocking the diffusing particles.

As seen from the Panels of Figures 1-3 the diffusing particles's energy considerably changes by merely passing through the trap. Thus, referring to the pair  $E^-(D_e, \frac{pc}{(1+c)}, p, t)$ ,  $E^-(D_e, p, p, t)$  one may realize the large change in kinetic energy the diffusing particles goes through upon passing from the left hand side to the right hand side of the trap. For example, comparing Panel 1 of Figure 1, which shows the energy  $E^-(D_e, \frac{pc}{(1+c)}, p, t)$  at the left hand side of the trap to Panel 1 of Figure 3 which shows the energy  $E^-(D_e, p, p, t)$  at the right hand side of this trap for the same values of  $c$ ,  $k$  and  $t$  one may realize that the particles's nonzero values of the energy changes upon diffusing through the trap from  $E \approx 10^4 \text{ erg}$  to  $E \approx 1 \text{ erg}$ . These large differences may be realized again by comparing Panel 1 in Figure 2, which shows the energy  $E^-(D_e, \frac{pc}{(1+c)}, p, t)$  at the left hand side of the trap to Panel 3 of Figure 3 which shows the energy  $E^-(D_e, p, p, t)$  at the right hand side of it for the same values of  $k$ ,  $c$  and  $t$ . As seen, the particles's nonzero values of the energy decreases upon passage of the trap from  $E \approx 10^4$  to  $E \approx 15$ . Thus, one may conclude that by diffusing through the traps the particles lose a huge amount of the energy they possess before the diffusion.

The time evolutions of the energies from Eqs (31)-(34) as functions of  $\kappa p$  reveal in a more pronounced way the mentioned large differences in the nonzero values of the energies. This is demonstrated in the first two Panels of Figure 4 which show the energies  $E^-(D_e, \frac{pc}{(1+c)}, p, t)$  and  $E^+(D_e, p, \frac{pc}{(1+c)}, t)$  for the 60 different values of  $t = 1 + n \cdot 0.5$ ,  $n = 1, 2, \dots, 59$  in each panel and for  $c = 2$  and  $k = 1$  for all the graphs shown. Note the giant differences of about  $10^{44}$  between the nonzero values of the energies in Panels 1-2. Continuing to increase  $t$  causes the energy in Panel 1 to grow (not shown) even beyond  $10^{80} \text{ erg}$ . Since these energies are not physically possible we conclude that there exist points along the  $\kappa p$  in which the energies  $E^-(D_e, \frac{pc}{(1+c)}, p, t)$  are not allowed for large values of the time  $t$ . In Panel 3 we show a three-dimensional surface of the energies  $E^-(D_e, p, p, t)$  as function of  $\kappa p$  and the time  $t$ . Note that it is constant with  $\kappa p$  and decreases to zero, in contrast to the energy from Panel 1, as  $t$  increases. Panel 4 shows the energy  $E^+(D_e, \frac{pc}{(1+c)}, \frac{pc}{(1+c)}, t)$ , as function of  $\kappa p$ , for the 20 values of  $t = 1 + n \cdot 0.5$ ,  $n = 0, 1, \dots, 19$  and for  $c = 2$  and  $k = 1$  for all the graphs. The

dense line just above the abscissa axis denote the higher values of  $t$  for which the constant values of the energy (as function of  $\kappa p$ ) tend, like those of Panel 3, to zero.

From the discussion thus far one may realize that generally the nonzero values of the energy  $E^-(D_e, \frac{pc}{(1+c)}, p, t)$  are greater by several order of magnitudes from the other three energies as shown by comparing the Panels of Figures 1, 2 and 4. These great differences are further pronounced for increasing values of the time as shown in the Panel 1 of Figure 3. But that is no more so when the time decreases as turns out (not shown) when the energies were calculated at small times. Thus, for example, decreasing the time from  $t \approx 30$  to  $t \approx 0.2$  causes the nonzero values of the energy  $E^-(D_e, \frac{pc}{(1+c)}, p, t)$  to decrease from about  $10^{44}$  *erg* (see Panels 1 of Figure 4) to about 100 *erg*. Likewise, the energy  $E^-(D_e, p, p, t)$  decreases from about 15 *erg* (see Panel 3 of Figure 3) for  $t = 2$  to 3 *erg* for  $t = 0.2$  (not shown).

## 6 Concluding Remarks

We have discussed, using the transfer matrix method, the energy of the particles which diffuse through the unbounded one-dimensional multitraps system. The classical initial and boundary value problem related to diffusion through an imperfect trap was adapted to apply to an infinite array of similar traps as done in the sets (1)-(3). Following the conventional transfer matrix procedure, which is used for discussing the quantum Kronig-Penney multibarrier array, we obtain a similar matrix equation (Eq (8)) which relates the imperfect traps across the whole array. Using, as for the analogous quantum multibarrier system, the periodicity of the array we obtain a quadratic characteristic equation (Eq (11)) for the two-dimensional matrix which relates the two faces of the general  $j - th$  trap. We solve this equation for the involved eigenvalues of this matrix and impose upon them the finiteness condition at the limit at which the number  $N$  of barriers becomes very large. As a result two inequalities (16)-(17) are obtained which are the central expressions from which we derive the appropri-



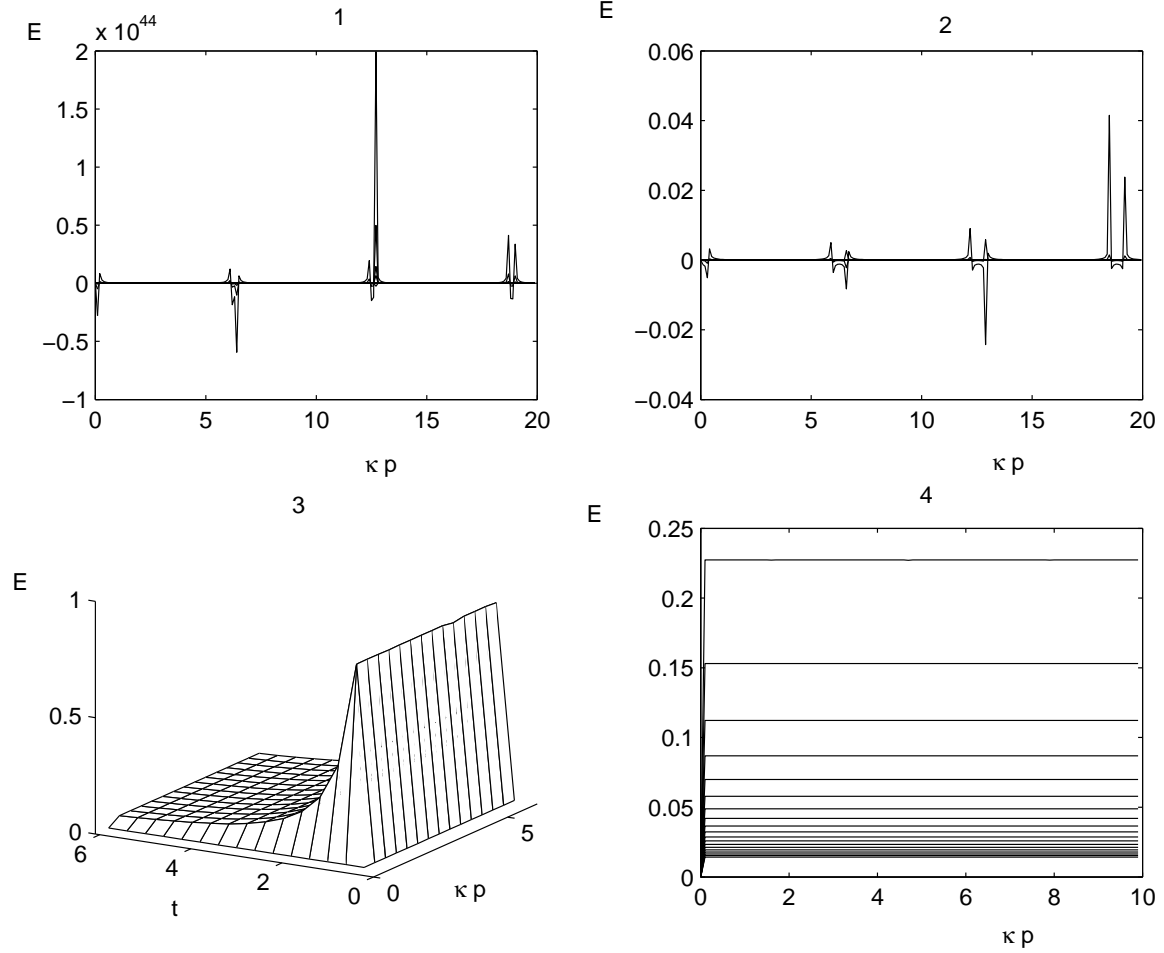


Figure 4: Panels 1 and 2 respectively show the energies  $E^-(D_e, \frac{pc}{(1+c)}, p, t)$  and  $E^+(D_e, p, \frac{pc}{(1+c)}, t)$  as functions of  $\kappa p$  for the 60 values of the time  $t = 1 + n \cdot 0.5$ ,  $n = 0, 1, 2, \dots, 59$ . One may realize that as the time grows the nonzero values of the energy  $E^-(D_e, \frac{pc}{(1+c)}, p, t)$  steeply increase. The ratio  $c$  and the trapping rate  $k$  for all the graphs of Panels 1-2 are  $c = 2$  and  $k = 1$ . Compared to the energy from Panel 1 which grows with  $t$  the energies  $E^-(D_e, p, p, t)$  and  $E^+(D_e, \frac{pc}{(1+c)}, \frac{pc}{(1+c)}, t)$  shown respectively in Panel 3 and 4 decrease with time to zero. Panel 4 is drawn for the 20 values of  $t = 1 + n \cdot 0.5$ ,  $n = 0, 1, 2, \dots, 19$  and for  $c = 2$  and  $k = 1$ . The upper lines in Panel 4 fit the small values of  $t$  and the lower lines fit the large values. The energies are given in units of *ergs*.

ate kinetic energies of the diffusing particles. Writing the matrix components  $T_{11}(\frac{pc}{(1+c)}, p)$  and  $T_{22}(\frac{pc}{(1+c)}, p)$  in these inequalities in terms of the appropriate energies (see Eqs (15)-(23) and discussion there) and using the properties of the transfer matrix method (see Eqs (18), (21) and (24)) we obtain two simultaneous equations involving two energies. We have found that each of these two energies is composed of two parts; one is related to the left hand face of the trap and the second to its right hand face. It is also found that the two parts of each of the two energies differ greatly from each other not only in value but also in the way they are expressed as functions of the related variables  $c$ ,  $k$ ,  $t$  and  $\kappa p$ . That is, as seen from Eqs (31)-(34) one part of each of these two energies is expressed in ideal trap terms only and the second part in imperfect trap terms only. These differences entail the results that by merely diffusing through the trap the particles's energy totally changes as realized from the appended figures. Moreover, there exist great variations not only between the two parts of the same energy but also between different sections (along the  $\kappa p$  axis) of the same part itself. For example, in the respective Panels 1 of Figures 1, 2 and 4 we have found that the energy  $E^-(D_e, \dot{x}_j^{left}, p, t)$  at the left hand face of the trap assumes values which greatly varies even in very short ranges of  $\kappa p$ .

As discussed in Section IV the points along the  $\kappa p$  axis at which the energies may assume unexpected, or even disallowed values, are related to the following two kinds of points; (1)  $\kappa p = \frac{\pi}{2} + n\pi$ ,  $n = 0, 1, 2, \dots$  (2)  $\kappa p = \text{arc}(\cos(\frac{A(\dot{x}_j^{right}, D_e)}{A(\dot{x}_j^{left}, D_e)}))$ . Another important variable which entails a large changes in the values of the energies is the time  $t$  as realized from the Panels of the appended Figures (see, especially, Panels 1-4 of Figure 4). The analytical expressions obtained are corroborated by the different attached figures.

As noted, the analogous discussion of the quantum Kronig-Penney multibarrier entails the finding of points along the corresponding  $\kappa p$  axis at which the energy is disallowed. Here, for the classical imperfect multitraps we have found corresponding disallowed energies which take the form of either negative values for the kinetic energy or of a discontinuous change of

this energy from zero to enormous positive values as in Panel 1 of Figure 4. The quantum band-gap structure found in the Kronig-Penney multibarrier array have been turned out to have great applications in wide areas of solid state physics such as semiconductor devices and computer chips. The striking similarity in the forms of the Schroedinger and diffusion equations as well as the common possibility to investigate and discuss them by the transfer matrix method may entail in the future similar successful development for the classical diffusive systems.

## APPENDIX A

### A The matrix elements from Eq (7)

The matrix elements  $T_{11}(\dot{x}_j^{left}, \dot{x}_j^{right})$ ,  $T_{12}(\dot{x}_j^{left}, \dot{x}_j^{right})$ ,  $T_{21}(\dot{x}_j^{left}, \dot{x}_j^{right})$ , and  $T_{22}(\dot{x}_j^{left}, \dot{x}_j^{right})$  of the two-dimensional matrix  $T^{(j)}$  from Eq (7) are fully discussed and derived in [6, 7] and are given by the following expressions

$$T_{11}(\dot{x}_j^{left}, \dot{x}_j^{right}) = \frac{\alpha(D_e, \dot{x}_j^{left}, \dot{x}_i, t)\alpha(D_i, \dot{x}_j^{right}, \dot{x}_i, t)}{\alpha(D_i, \dot{x}_j^{left}, \dot{x}_i, t)\alpha(D_e, \dot{x}_j^{right}, \dot{x}_i, t)}, \quad 1 \leq j \leq N \quad (A_1)$$

$$T_{12}(\dot{x}_j^{left}, \dot{x}_j^{right}) = 0, \quad 1 \leq j \leq N \quad (A_2)$$

$$\begin{aligned} T_{21}(\dot{x}_j^{left}, \dot{x}_j^{right}) = & \rho_0 \left( \frac{\eta(D_i, \dot{x}_j^{right}, t)}{\eta(D_e, \dot{x}_j^{right}, t)} \left( \frac{\xi(D_e, \dot{x}_j^{left}, \dot{x}_i, t)}{\eta(D_i, \dot{x}_j^{left}, t)} - \right. \right. \\ & \left. \left. - \frac{\alpha(D_e, \dot{x}_j^{left}, \dot{x}_i, t)\xi(D_i, \dot{x}_j^{left}, \dot{x}_i, t)}{\alpha(D_i, \dot{x}_j^{left}, \dot{x}_i, t)\eta(D_i, \dot{x}_j^{left}, t)} \right) \right) + \\ & + \frac{\alpha(D_e, \dot{x}_j^{left}, \dot{x}_i, t)}{\alpha(D_i, \dot{x}_j^{left}, \dot{x}_i, t)} \left( \frac{\xi(D_i, \dot{x}_j^{right}, \dot{x}_i, t)}{\eta(D_e, \dot{x}_j^{right}, t)} - \right. \\ & \left. - \frac{\alpha(D_i, \dot{x}_j^{right}, \dot{x}_i, t)\xi(D_e, \dot{x}_j^{right}, \dot{x}_i, t)}{\alpha(D_e, \dot{x}_j^{right}, \dot{x}_i, t)\eta(D_e, \dot{x}_j^{right}, t)} \right), \quad 1 \leq j \leq N \end{aligned} \quad (A_3)$$

$$T_{22}(\dot{x}_j^{left}, \dot{x}_j^{right}) = \frac{\eta(D_e, \dot{x}_j^{left}, t)\eta(D_i, \dot{x}_j^{right}, t)}{\eta(D_i, \dot{x}_j^{left}, t)\eta(D_e, \dot{x}_j^{right}, t)}, \quad 1 \leq j \leq N \quad (A_4)$$

The parameters  $\alpha$ ,  $\xi$ , and  $\eta$  are given by (we write these expression for  $D_e$  and  $x = \dot{x}_j^{left}$ )

$$\begin{aligned} \alpha(D_e, \dot{x}_j^{left}, \dot{x}_i, t) &= erf\left(\frac{(\dot{x}_j^{left} - \dot{x}_i)}{2\sqrt{D_e t}}\right) + \exp(k^2 D_e t + k(\dot{x}_j^{left} - \dot{x}_i)) \cdot \\ &\cdot erf\left(k\sqrt{D_e t} + \frac{(\dot{x}_j^{left} - \dot{x}_i)}{2\sqrt{D_e t}}\right) \end{aligned} \quad (A_5)$$

$$\xi(D_e, \dot{x}_j^{left}, \dot{x}_i, t) = k \exp(k^2 D_e t + k(\dot{x}_j^{left} - \dot{x}_i)) erf\left(k\sqrt{D_e t} + \frac{(\dot{x}_j^{left} - \dot{x}_i)}{2\sqrt{D_e t}}\right) \quad (A_6)$$

$$\eta(D_e, \dot{x}_i, t) = -\frac{\pi}{\dot{x}_i} e^{-\left(\frac{\pi}{\dot{x}_i}\right)^2 D_e t} \quad (A_7)$$

Note that in [6, 7] the variables  $\dot{x}_i$  are not subtracted from the variables  $\dot{x}_j$  in the functions  $\alpha$  and  $\xi$ . This is because the presence or absence of this subtraction do not affect at all the values of the matrix elements  $T_{11}$  and  $T_{22}$  as may be realized from their definitions in Eqs (A<sub>1</sub>) and (A<sub>4</sub>) in this Appendix. Also, in [6, 7] we discuss the whole array of the bounded dense multitraps in which case the variables  $\dot{x}_i$  and  $\dot{x}_j$  do not, necessarily, refer to the same trap and so this subtraction is ignored there. Here, on the other hand, the variables  $\dot{x}_i$  and  $\dot{x}_j$  refer to the same trap which represents the unbounded multitraps system and so the expression  $(\dot{x}_j - \dot{x}_i)$  should not be approximated to  $\dot{x}_j$ .

## APPENDIX B

### B The solutions of the simultaneous Eqs (25)-(26)

We solve in this Appendix the two Eqs (25)-(26) for the energies  $E(D_e, \frac{pc}{(1+c)}, \dot{x}_i, t)$  and  $E(D_e, p, \dot{x}_i, t)$ . We begin by solving Eq (25) for  $E(D_e, \frac{pc}{(1+c)}, \dot{x}_i, t)$  in terms of  $E(D_e, p, \dot{x}_i, t)$  and then we substitute this solution in Eq (26) and solve it for  $E(D_e, p, \dot{x}_i, t)$ . In order not to be involved with cumbersome expressions we define the following quantities

$$\begin{aligned}
 X_1 &= \frac{A(\frac{pc}{(1+c)}, D_e)}{A(p, D_e)} \cdot \cos(\kappa p) \\
 X_2 &= D_e B(\frac{pc}{(1+c)}, D_i) \rho_2(D_i, \frac{pc}{(1+c)}, \dot{x}_i, t) \\
 X_3 &= D_e B(\frac{pc}{(1+c)}, D_e) \rho_2(D_e, \frac{pc}{(1+c)}, \dot{x}_i, t) \\
 X_4 &= D_e B(p, D_e) \rho_2(D_e, p, \dot{x}_i, t) \\
 X_5 &= D_e B(p, D_i) \rho_2(D_i, p, \dot{x}_i, t)
 \end{aligned} \tag{B1}$$

Substituting the last quantities in Eq (25) we obtain

$$\begin{aligned}
 t^2(1 - X_1)E(D_e, \frac{pc}{(1+c)}, \dot{x}_i, t)E(D_e, p, \dot{x}_i, t) - t \left( E(D_e, \frac{pc}{(1+c)}, \dot{x}_i, t)(X_5 - X_4X_1) + \right. \\
 \left. + E(D_e, p, \dot{x}_i, t)(X_3 - X_2X_1) \right) + X_3X_5 - X_2X_4X_1 = 0
 \end{aligned} \tag{B2}$$

Solving the last equation for  $E(D_e, \frac{pc}{(1+c)}, \dot{x}_i, t)$  we obtain

$$E(D_e, \frac{pc}{(1+c)}, \dot{x}_i, t) = \frac{X_1X_2(X_4 - tE(D_e, p, \dot{x}_i, t)) - X_3(X_5 - tE(D_e, p, \dot{x}_i, t))}{tX_1(X_4 - tE(D_e, p, \dot{x}_i, t)) - t(X_5 - tE(D_e, p, \dot{x}_i, t))} \tag{B3}$$

We may now substitute the last expression for  $E(D_e, \frac{pc}{(1+c)}, \dot{x}_i, t)$  in Eq (26) and solve it for  $E(D_e, p, \dot{x}_i, t)$ . But before proceeding we define the following quantities

$$\begin{aligned}
Y_1 &= t^2 \left( \frac{B(p, D_e)}{B(\frac{pc}{(1+c)}, D_e)} - \cos(\kappa p) \right) \\
Y_2 &= t D_e \left( \frac{B(p, D_e)}{B(\frac{pc}{(1+c)}, D_e)} A(p, D_i) \alpha(D_i, p, \dot{x}_i, t) - A(p, D_e) \alpha(D_e, p, \dot{x}_i, t) \cos(\kappa p) \right) \\
Y_3 &= t D_e \left( \frac{B(p, D_e)}{B(\frac{pc}{(1+c)}, D_e)} A(\frac{pc}{(1+c)}, D_e) \alpha(D_e, \frac{pc}{(1+c)}, \dot{x}_i, t) - A(\frac{pc}{(1+c)}, D_i) \cdot \right. \\
&\quad \left. \cdot \alpha(D_i, \frac{pc}{(1+c)}, \dot{x}_i, t) \cos(\kappa p) \right) \tag{B4} \\
Y_4 &= D_e^2 \frac{B(p, D_e)}{B(\frac{pc}{(1+c)}, D_e)} A(p, D_i) \alpha(D_i, p, \dot{x}_i, t) A(\frac{pc}{(1+c)}, D_e) \alpha(D_e, \frac{pc}{(1+c)}, \dot{x}_i, t) \\
Y_5 &= D_e^2 A(p, D_e) \alpha(D_e, p, \dot{x}_i, t) A(\frac{pc}{(1+c)}, D_i) \alpha(D_i, \frac{pc}{(1+c)}, \dot{x}_i, t) \cos(\kappa p)
\end{aligned}$$

Substituting from Eqs (B3)-(B4) in Eq (26) and rearranging we obtain the following quadratic equation for  $E(D_e, p, \dot{x}_i, t)$

$$\begin{aligned}
&E^2(D_e, p, \dot{x}_i, t) \left( (tX_3 - tX_1X_2)Y_1 - t^2(1 - X_1)Y_3 \right) + E(D_e, p, \dot{x}_i, t) \cdot \\
&\cdot \left\{ (t^2(1 - X_1)(Y_4 - Y_5) - (tX_4X_1 - tX_5)Y_3 - t(X_3 - X_1X_2)Y_2 + (X_4X_1X_2 - \right. \\
&\quad \left. - X_3X_5)Y_1 \right\} - (X_4X_1X_2 - X_3X_5)Y_2 + t(X_4X_1 - X_5)(Y_4 - Y_5) = 0 \tag{B5}
\end{aligned}$$

The two solutions of the last quadratic equation are

$$E^+(D_e, p, \dot{x}_i, t) = \frac{t(X_1X_4 - X_5)Y_3 - (X_1X_2X_4 - X_3X_5)Y_1}{(tX_3 - tX_1X_2)Y_1 - t^2(1 - X_1)Y_3} \tag{B6}$$

$$E^-(D_e, p, \dot{x}_i, t) = \frac{(X_3 - X_1X_2)Y_2 - t(1 - X_1)(Y_4 - Y_5)}{(X_3 - X_1X_2)Y_1 - t(1 - X_1)Y_3} = \frac{Y_2}{Y_1}, \tag{B7}$$

where the last result for  $E^-(D_e, p, \dot{x}_i, t)$  is obtained by using Eqs (B<sub>4</sub>). The two expressions from (B<sub>6</sub>)-(B<sub>7</sub>) are the energies at the right hand side of the trap. The corresponding energies  $E^\pm(D_e, \frac{pc}{(1+c)}, \dot{x}_i, t)$  at the left hand side of it may be obtained from Eq (B<sub>3</sub>) by substituting in it for  $E^\pm(D_e, p, \dot{x}_i, t)$  from Eqs (B<sub>6</sub>)-(eB<sub>7</sub>). Thus, using Eq (B<sub>6</sub>) one may find  $E^+(D_e, \frac{pc}{(1+c)}, \dot{x}_i, t)$  as

$$E^+(D_e, \frac{pc}{(1+c)}, \dot{x}_i, t) = \frac{Y_3}{Y_1} \quad (B_8)$$

where use is made of the first and third of Eqs (B<sub>4</sub>). The second energy  $E^-(D_e, \frac{pc}{(1+c)}, \dot{x}_i, t)$  is obtained by substituting from Eq (B<sub>7</sub>) in Eq (B<sub>3</sub>).

$$E^-(D_e, \frac{pc}{(1+c)}, \dot{x}_i, t) = \quad (B_9)$$

$$= \frac{(X_3 - X_1 X_2)((tX_3 - tX_1 X_2)Y_2 + (X_1 X_2 X_4 - X_3 X_5)Y_1) - (1 - X_1)(t^2(X_3 - X_1 X_2)(Y_4 - Y_5) + t(X_1 X_2 X_4 - X_3 X_5)Y_3)}{(X_3 - X_1 X_2)((t^2(1 - X_1)Y_2 + t(X_1 X_4 - X_5)Y_1) - (1 - X_1)(t^3(1 - X_1)(Y_4 - Y_5) + t^2(X_1 X_4 - X_5)Y_3))}$$

## References

- [1] D. C. Mattis and M. L. Glasser, Rev. Mod. Phys, **70**, 979-1001 (1998).
- [2] G. Roepstorff, "Path integral approach to quantumk physics", Springer-Verlag (1994).
- [3] E. Merzbacher, "Quantum mechanics" second edition, Wiley (1961).
- [4] C. C. Tannoudji, B. Diu, And Franck Laloe, "Quantum mechanics", Wiley (1977)
- [5] K. W. Yu, Computers in Physics, **4**, 176-178 (1990)
- [6] D. Bar, Phys. Rev E, **64**, 026108 (2001); D. Bar, Phys. Rev E, **67**, 056123 (2003).
- [7] D. Bar, Phys. Rev E, **70**, 016607 (2004)

- [8] R. V. Smoluchowski, *Z. Phys. Chem., Stoechiom. Verwandtschaftsl.*, **29**, 129 (1917)
- [9] G. Abramson and H. Wio, *Chaos. Solitons. Fractals*, **6**, 1 (1995); S. Torquato and C. Yeong, *J. Chem. Phys.*, **106**, 8814 (1997); A. Giacometti and H. Nakanishi, *Phys. Rev E*, **50**, 1093 (1994); T. Nieuwenhuize and H. Brandt, *J. Stat. Phys.*, **59**, 53 (1990).
- [10] R. M. Noyes, *J. Chem. Phys.*, **22**, 1349 (1954)
- [11] D. Ben-Avraham And S. Havlin, "Diffusion and reactions in fractals and disordered media" Cambridge, Cambridge university press (2000); G. S. Weiss, R. Kopelman and S. Havlin, *Phys. Rev A*, **39**, 466 (1989).
- [12] F. C. Collins and G. E. Kimball, *J. Colloid Sci.*, **4**, 425 (1949)
- [13] M. A. Re and C. E. Budde, *Phys. Rev. E* **61**, 2, 1110-1120 (2000).
- [14] C. A. Condat, G. Sibona and C. E. Budde, *Phys. Rev E*, **51**, 2839-2843 (1995).
- [15] H. Taitelbaum, R. Kopelman, G. H. Weiss and S. Havlin, *Phys. Rev A*, **41**, 3116, (1990); H. Taitelbaum, *Phys. Rev A*, **43**, 6592 (1991).
- [16] J. T. Chuang and K. B. Eisenthal, *J. Chem. Phys.*, **62**, 2213 (1975)
- [17] W. Nadler and D. L. Stein, *J. Chem. Phys.*, **104**, 1918 (1996)
- [18] C. Kittel, "Introduction to solid state physics", Sixth Edition, , Wiley, New York, (1986).
- [19] N. Ashcroft, N. D. Mermin and D. Mermin, "Solid state physic", International Thomson Publishing, (1976)
- [20] Rene Denne Meyer, "Introduction to partial differential equations and boudary values problems", McGraw-Hill, New York (1968)
- [21] F. Reif, "Statistical Physics" (McGraw-Hill, New-York (1965))



[22] Y. Varbin and G. Sela, "Statistical Physics", Volume 1, (Hebrew Edition), Open University Press, Tel Aviv, Israel 1992,